

ΛNN and ΣNN systems at threshold

H. Garcilazo^(1,3), T. Fernández-Caramés⁽²⁾, and A. Valcarce⁽³⁾

(1) *Escuela Superior de Física y Matemáticas, Instituto Politécnico Nacional, Edificio 9, 07738 México D.F., Mexico*

(2) *Departamento de Física Teórica e IFIC, Universidad de Valencia - CSIC, E-46100 Burjassot, Valencia, Spain*

(3) *Departamento de Física Fundamental e IUFFyM, Universidad de Salamanca, E-37008 Salamanca, Spain*

Abstract

We calculate the hypertriton binding energy and the Λd and Σd scattering lengths using baryon-baryon interactions obtained from a chiral constituent quark model. We study consistently the ΛNN and ΣNN systems analyzing the effect of the $\Sigma \leftrightarrow \Lambda$ conversion. Our interactions correctly predict the hypertriton binding energy. The $(I, J) = (0, 3/2)$ ΛNN channel is also attractive and it might have a bound state. From the condition of nonexistence of a $(0, 3/2)$ ΛNN bound state, an upper limit for the spin-triplet ΛN scattering length is obtained. We also present results for the elastic and inelastic ΣN and ΛN cross sections. The consistent description of the ΣN scattering cross sections imposes a lower limit for the corresponding spin-triplet scattering lengths. In the ΣNN system the only attractive channels are $(I, J) = (1, 1/2)$ and $(0, 1/2)$, the $(1, 1/2)$ state being the most attractive one.

arXiv:hep-ph/0701275v1 31 Jan 2007

I. INTRODUCTION

The deuteron plays an important role in conventional nonstrange nuclear physics by constraining our models of the nucleon-nucleon (NN) force. This is a consequence of the precision with which we can measure properties of a bound system, exceeding by far that possible in measurements of the scattering amplitudes. Because neither the ΛN nor the ΣN (spin-triplet or spin-singlet) interactions possess sufficient strength to support a bound state, it is the hypertriton that plays the important role of the deuteron in hypernuclear physics. It is therefore the ground state of the ΛNN system ($J^P = 1/2^+, I = 0$), that must be used to constrain our models of the hyperon-nucleon (YN) force. In fact, the rather small binding energy of the hypertriton turned out to be elusive for different meson-theoretical interactions [1,2].

Unfortunately, there is hardly any scattering data available for the hyperon-nucleon (YN) system. The sparse database for ΛN and ΣN scattering and reactions is inadequate to fully determine the YN interactions. Therefore, interaction models are generally constrained by flavor $SU(3)$ symmetry. In this spirit, one meson-exchange [3] and quark-model based [4] forces have been developed which are all consistent with the scarce YN database.

The chiral constituent quark model has been very successful in the simultaneous description of the baryon-baryon interaction and the baryon spectrum as well as in the study of the two- and three-baryon bound-state problem for the nonstrange sector [5]. A simple generalization of this model to the strange sector has also been recently applied to study the meson and baryon spectra [6] and the ΣNN bound-state problem [7]. In this last work we solved the Faddeev equations of the coupled $\Sigma NN - \Lambda NN$ system below the Σd threshold in order to study the amount of attraction present in the different isospin-spin channels (I, J).

In this work, we will continue our study of the strangeness $\hat{S} = -1$ three-baryon systems by considering also the region of ΛNN bound states, where the hypertriton lies, and calculating for the first time the Λd and Σd scattering lengths. In the past the question was posed whether other states than that of the hypertriton, and in particular the $(I, J) = (0, 3/2)$, could also be bound. We shall investigate this question by studying simultaneously all ΛNN and ΣNN states with $J = 1/2, 3/2$ and $I = 0, 1, 2$. We will also ask not only for the description of the elastic ΛN cross section, but also for the elastic and inelastic ΣN cross sections. Therefore we pursue a simultaneous description of almost all experimentally available observables in the two- and three-baryon systems with strangeness $\hat{S} = -1$. The set of observables used would put stringent conditions to any potential model approach. In particular, this study will provide with a powerful tool to determine the relative strength of the spin-singlet and spin-triplet hyperon-nucleon interactions, allowing to refine details on the model interaction.

The paper is organized as follows. Our formalism for the baryon-baryon interactions and the Faddeev equations for the bound-state problem of the coupled $\Sigma NN - \Lambda NN$ system has been already presented in Ref. [7]. Thus in the next section we will resume some relevant aspects of the interacting potential as well as we will present the corresponding equations for Λd and Σd scattering at threshold and the expressions for the scattering lengths. Section III will be devoted to present and discuss the results obtained. Finally, in section IV we will resume our most relevant conclusions.

II. FORMALISM

A. The two-body interactions

The baryon-baryon interactions involved in the study of the coupled $\Sigma NN - \Lambda NN$ system are obtained from the chiral constituent quark model [5,6]. In this model baryons are described as clusters of three interacting massive (constituent) quarks, the mass coming from the spontaneous breaking of chiral symmetry. The first ingredient of the quark-quark interaction is a confining potential (*CON*). Perturbative aspects of QCD are taken into account by means of a one-gluon potential (*OGE*). Spontaneous breaking of chiral symmetry gives rise to boson exchanges between quarks. In particular, there appear pseudoscalar boson exchanges, that have already been considered in our model [7], and their corresponding scalar partners: σ , κ , f_0 and a_0 . In our previous study of the baryon-baryon interaction for systems with strangeness, the scalar meson-exchange potential was used as in the nonstrange systems, i.e. only σ -meson exchange. Here we first analyze the effect of the inclusion of the other scalars of the octet. These scalar potentials have the same functional form and a different $SU(3)$ operatorial dependence, i.e.,

$$V(\vec{r}_{ij}) = V_{a_0}(\vec{r}_{ij}) \sum_{F=1}^3 \lambda_i^F \cdot \lambda_j^F + V_{\kappa}(\vec{r}_{ij}) \sum_{F=4}^7 \lambda_i^F \cdot \lambda_j^F + V_{f_0}(\vec{r}_{ij}) \lambda_i^8 \cdot \lambda_j^8 + V_{\sigma}(\vec{r}_{ij}) \lambda_i^0 \cdot \lambda_j^0 \quad (1)$$

where

$$V_k(\vec{r}_{ij}) = -\frac{g_{ch}}{4\pi} \frac{\Lambda_k^2}{\Lambda_k^2 - m_k^2} m_k \left[Y(m_k r_{ij}) - \frac{\Lambda_k}{m_k} Y(\Lambda_k r_{ij}) \right], \quad (2)$$

with $k = a_0, \kappa, f_0$ or σ , and g_{ch} is the quark-meson coupling constant [5]. We give in Table I the expectation value of the different flavor operators appearing in Eq. (1) for the different two-body systems involved in our problem. If one takes additionally into account the smallness of the scalar mixing angle [8], one concludes that the f_0 meson does not contribute. Thus, there are two novelties when considering the full $SU(3)$ scalar octet. Firstly, a reduction in the strength of the σ -meson exchange potential, and second an increase of the attraction for spin-singlet and a decrease for spin-triplet channels mainly due to the κ -meson exchange. As a consequence, the effect of the scalar octet can be effectively taken into account by using a single scalar exchange of the form [9],

$$V_s(\vec{r}_{ij}) = -\frac{g_{ch}}{4\pi} \frac{\Lambda_s^2}{\Lambda_s^2 - m_s^2} m_s \left[Y(m_s r_{ij}) - \frac{\Lambda_s}{m_s} Y(\Lambda_s r_{ij}) \right], \quad (3)$$

with different parametrization for spin-singlet and spin-triplet channels. A parametrization of the full scalar octet exchange potential is obtained using the parameters given in Table II.

Finally, the quark-quark interaction will read:

$$V_{qq}(\vec{r}_{ij}) = V_{CON}(\vec{r}_{ij}) + V_{OGE}(\vec{r}_{ij}) + V_{\chi}(\vec{r}_{ij}) + V_s(\vec{r}_{ij}), \quad (4)$$

where the i and j indices are associated with i and j quarks respectively, \vec{r}_{ij} stands for the interquark distance, V_{χ} denotes the pseudoscalar meson-exchange interactions discussed in

Refs. [6,7], and V_s stands for the effective scalar meson-exchange potential just described. Explicit expression of all the interacting potentials and a more detailed discussion of the model can be found in Ref. [6]. In order to derive the local $NB_1 \rightarrow NB_2$ interactions from the basic qq interaction defined above we use a Born-Oppenheimer approximation. Explicitly, the potential is calculated as follows,

$$V_{NB_1(LST) \rightarrow NB_2(L'S'T)}(R) = \xi_{LST}^{L'S'T}(R) - \xi_{LST}^{L'S'T}(\infty), \quad (5)$$

where

$$\xi_{LST}^{L'S'T}(R) = \frac{\langle \Psi_{NB_2}^{L'S'T}(\vec{R}) | \sum_{i < j=1}^6 V_{qq}(\vec{r}_{ij}) | \Psi_{NB_1}^{LST}(\vec{R}) \rangle}{\sqrt{\langle \Psi_{NB_2}^{L'S'T}(\vec{R}) | \Psi_{NB_2}^{L'S'T}(\vec{R}) \rangle} \sqrt{\langle \Psi_{NB_1}^{LST}(\vec{R}) | \Psi_{NB_1}^{LST}(\vec{R}) \rangle}}. \quad (6)$$

In the last expression the quark coordinates are integrated out keeping R fixed, the resulting interaction being a function of the $N - B_i$ relative distance. The wave function $\Psi_{NB_i}^{LST}(\vec{R})$ for the two-baryon system is discussed in detail in Ref. [5].

B. Σd and Λd scattering at threshold

Our method [7] to transform the Faddeev equations from being integral equations in two continuous variables into integral equations in just one continuous variable is based in the expansion of the two-body t -matrices

$$t_{i;s_i i}(p_i, p'_i; e) = \sum_{nr} P_n(x_i) \tau_{i;s_i i}^{nr}(e) P_r(x'_i), \quad (7)$$

where P_n and P_r are Legendre polynomials,

$$x_i = \frac{p_i - b}{p_i + b}, \quad (8)$$

$$x'_i = \frac{p'_i - b}{p'_i + b}, \quad (9)$$

and p_i and p'_i are the initial and final relative momenta of the pair jk while b is a scale parameter of which the results do not depend on.

Following the same notation as in Ref. [7], where particle 1 is the hyperon and particles 2 and 3 are the two nucleons, the integral equations for βd scattering at threshold with $\beta = \Sigma$ or Λ are in the case of pure S -wave configurations,

$$\begin{aligned} T_{2;SI;\beta}^{ns_2 i_2}(q_2) &= B_{2;SI;\beta}^{ns_2 i_2}(q_2) + \sum_{ms_3 i_3} \int_0^\infty dq_3 \left[(-1)^{1+\sigma_1+\sigma_3-s_2+\tau_1+\tau_3-i_2} A_{23;SI}^{ns_2 i_2 ms_3 i_3}(q_2, q_3; E) \right. \\ &\quad \left. + 2 \sum_{rs_1 i_1} \int_0^\infty dq_1 A_{31;SI}^{ns_2 i_2 rs_1 i_1}(q_2, q_1; E) A_{13;SI}^{rs_1 i_1 ms_3 i_3}(q_1, q_3; E) \right] T_{2;SI}^{ms_3 i_3}(q_3), \quad (10) \end{aligned}$$

where σ_1 (τ_1) and σ_3 (τ_3) stand for the spin (isospin) of the hyperon and the nucleon respectively while s_i and i_i are the spin and isospin of the pair jk . $T_{2;SI;\beta}^{ns_2i_2}(q_2)$ is a two-component vector

$$T_{2;SI;\beta}^{ns_2i_2}(q_2) = \begin{pmatrix} T_{2;SI;\Sigma\beta}^{ns_2i_2}(q_2) \\ T_{2;SI;\Lambda\beta}^{ns_2i_2}(q_2) \end{pmatrix}, \quad (11)$$

while the kernel of Eq. (10) is a 2×2 matrix defined by

$$A_{23;SI}^{ns_2i_2ms_3i_3}(q_2, q_3; E) = \begin{pmatrix} A_{23;SI;\Sigma\Sigma}^{ns_2i_2ms_3i_3}(q_2, q_3; E) & A_{23;SI;\Sigma\Lambda}^{ns_2i_2ms_3i_3}(q_2, q_3; E) \\ A_{23;SI;\Lambda\Sigma}^{ns_2i_2ms_3i_3}(q_2, q_3; E) & A_{23;SI;\Lambda\Lambda}^{ns_2i_2ms_3i_3}(q_2, q_3; E) \end{pmatrix}, \quad (12)$$

$$A_{31;SI}^{ns_2i_2rs_1i_1}(q_2, q_1; E) = \begin{pmatrix} A_{31;SI;\Sigma N(\Sigma)}^{ns_2i_2rs_1i_1}(q_2, q_1; E) & A_{31;SI;\Sigma N(\Lambda)}^{ns_2i_2rs_1i_1}(q_2, q_1; E) \\ A_{31;SI;\Lambda N(\Sigma)}^{ns_2i_2rs_1i_1}(q_2, q_1; E) & A_{31;SI;\Lambda N(\Lambda)}^{ns_2i_2rs_1i_1}(q_2, q_1; E) \end{pmatrix}, \quad (13)$$

$$A_{13;SI}^{rs_1i_1ms_3i_3}(q_1, q_3; E) = \begin{pmatrix} A_{13;SI;N\Sigma}^{rs_1i_1ms_3i_3}(q_1, q_3; E) & 0 \\ 0 & A_{13;SI;N\Lambda}^{rs_1i_1ms_3i_3}(q_1, q_3; E) \end{pmatrix}, \quad (14)$$

where

$$A_{23;SI;\alpha\beta}^{ns_2i_2ms_3i_3}(q_2, q_3; E) = h_{23;SI}^{s_2i_2s_3i_3} \sum_r \tau_{2;s_2i_2;\alpha\beta}^{nr}(E - q_2^2/2\nu_2) \frac{q_3^2}{2} \\ \times \int_{-1}^1 d\cos\theta \frac{P_r(x'_2)P_m(x_3)}{E + \Delta E\delta_{\beta\Lambda} - p_3^2/2\mu_3 - q_3^2/2\nu_3 + i\epsilon}; \quad \alpha, \beta = \Sigma, \Lambda, \quad (15)$$

$$A_{31;SI;\alpha N(\beta)}^{ns_2i_2ms_1i_1}(q_2, q_1; E) = h_{31;SI}^{s_2i_2s_1i_1} \sum_r \tau_{3;s_2i_2;\alpha\beta}^{nr}(E - q_2^2/2\nu_2) \frac{q_1^2}{2} \\ \times \int_{-1}^1 d\cos\theta \frac{P_r(x'_3)P_m(x_1)}{E + \Delta E\delta_{\beta\Lambda} - p_1^2/2\mu_1 - q_1^2/2\nu_1 + i\epsilon}; \quad \alpha, \beta = \Sigma, \Lambda, \quad (16)$$

$$A_{13;SI;N\beta}^{ns_1i_1ms_3i_3}(q_1, q_3; E) = h_{13;SI}^{s_1i_1s_3i_3} \sum_r \tau_{1;s_1i_1;N\beta}^{nr}(E + \Delta E\delta_{\beta\Lambda} - q_1^2/2\nu_1) \frac{q_3^2}{2} \\ \times \int_{-1}^1 d\cos\theta \frac{P_r(x'_1)P_m(x_3)}{E + \Delta E\delta_{\beta\Lambda} - p_3^2/2\mu_3 - q_3^2/2\nu_3 + i\epsilon}; \quad \beta = \Sigma, \Lambda, \quad (17)$$

with the isospin and mass of particle 1 (the hyperon) being determined by the subindex β . μ_i and ν_i are the usual reduced masses and the subindex $\alpha N(\beta)$ in Eq. (16) indicates a transition $\alpha N \rightarrow \beta N$ with a nucleon as spectator followed by a $NN \rightarrow NN$ transition with β as spectator. $\tau_{2;s_2i_2;\alpha\beta}^{nr}(e)$ are the coefficients of the expansion in terms of Legendre polynomials of the hyperon-nucleon t -matrix $t_{2;s_2i_2;\alpha\beta}(p_2, p'_2; e)$ for the transition $\alpha N \rightarrow \beta N$, i.e.,

$$\tau_{i;s_ii_i;\alpha\beta}^{nr}(e) = \frac{2n+1}{2} \frac{2r+1}{2} \int_{-1}^1 dx_i \int_{-1}^1 dx'_i P_n(x_i) t_{i;s_ii_i;\alpha\beta}(p_i, p'_i; e) P_r(x'_i). \quad (18)$$

The energy shift ΔE , which is usually taken as $M_\alpha - M_\beta$, will be chosen instead such that at the βd threshold the momentum of the αd system has the correct value, i.e.,

$$\Delta E = \frac{[(m_\beta + m_d)^2 - (m_\alpha + m_d)^2][(m_\beta + m_d)^2 - (m_\alpha - m_d)^2]}{8\mu_{\alpha d}(m_\beta + m_d)^2}, \quad (19)$$

where $\mu_{\alpha d}$ is the αd reduced mass.

The inhomogeneous term of Eq. (10), $B_{2;SI;\beta}^{ns_2i_2}(q_2)$ is a two-component vector

$$B_{2;SI;\beta}^{ns_2i_2}(q_2) = \begin{pmatrix} B_{2;SI;\Sigma\beta}^{ns_2i_2}(q_2) \\ B_{2;SI;\Lambda\beta}^{ns_2i_2}(q_2) \end{pmatrix}, \quad (20)$$

where

$$B_{2;SI;\alpha\beta}^{ns_2i_2}(q_2) = h_{31;SI}^{s_2i_210} \phi_d(q_2) \sum_r \tau_{2;s_2i_2;\alpha\beta}^{nr} (E_\beta^{th} - q_2^2/2\nu_2) P_r(x'_2). \quad (21)$$

$h_{31;SI}^{s_2i_2s_1i_1}$ with $s_1 = 1$ and $i_1 = 0$ are the spin-isospin transition coefficients corresponding to a hyperon-deuteron initial state (see Eq. (30), of Ref. [7]), $\phi_d(q_2)$ is the deuteron wave function, E_β^{th} is the energy of the βd threshold, $P_r(x'_2)$ is a Legendre polynomial of order r , and

$$x'_2 = \frac{\frac{\eta_2}{m_3} q_2 - b}{\frac{\eta_2}{m_3} q_2 + b}. \quad (22)$$

Finally, after solving the inhomogeneous set of equations (10), the βd scattering length is given by

$$A_{\beta d} = -\pi\mu_{\beta d} T_{\beta\beta}, \quad (23)$$

with

$$T_{\beta\beta} = 2 \sum_{ns_2i_2} h_{13;SI}^{10s_2i_2} \int_0^\infty q_2^2 dq_2 \phi_d(q_2) P_n(x'_2) T_{2;SI;\beta\beta}^{ns_2i_2}(q_2). \quad (24)$$

In the case of the ΣNN system, even for energies below the Σd threshold, one encounters the three-body singularities of the ΛNN system so that to solve the integral equations (10) one has to use the contour rotation method where the momenta are rotated into the complex plane $q_i \rightarrow q_i e^{-i\phi}$ since as pointed out in Ref. [7] the results do not depend on the contour rotation angle ϕ .

III. RESULTS

In order to solve the integral equations (10) for the coupled $\Sigma NN - \Lambda NN$ system we consider all configurations where the baryon-baryon subsystems are in an S -wave and the third particle is also in an S -wave with respect to the pair. However, to construct the two-body t -matrices that serve as input of the Faddeev equations we considered the full interaction including the contribution of the D -waves and of course the coupling between

the ΣN and ΛN subsystems (this is known as the truncated t -matrix approximation [10]). We give in Table III the two-body channels that are included in our calculation. For a given three-body state (I, J) the number of two-body channels that enter is determined by the triangle selection rules $|J - \frac{1}{2}| \leq s_i \leq J + \frac{1}{2}$ and $|I - \frac{1}{2}| \leq i_i \leq I + \frac{1}{2}$. For the parameter b in Eqs. (8) and (9) we found that $b = 3 \text{ fm}^{-1}$ leads to very stable results while for the expansion (7) we took twelve Legendre polynomials, i.e., $0 \leq n \leq 11$.

The results of our model correspond to the first line of Tables IV, V, and VI. In order to study their dependence on the strength of the spin-singlet and spin-triplet hyperon-nucleon interactions, we will construct different families of interacting potentials by introducing small variations of the parameters of the effective scalar exchange potential around our reference values given in Table II. These families are resummed in Table IV and they are characterized by their ΛN , $a_{i,s}$, and ΣN , $a'_{i,s}$, scattering lengths. The ΣN scattering lengths $a'_{1/2,s}$ are complex since for these quantum numbers the ΛN channel is always open. Under the first row of Table IV, we give in parenthesis the scattering length of the hyperon-nucleon channels as reproduced by the expansion (7) in order to see how much they deviate from the exact values. As one can see, the deviations are typically of the order of 1%. We show in Fig. 1 the cross sections near threshold of the five hyperon-nucleon processes for which data are available and compare them with the predictions of our model with the scalar mesons taken as indicated in Table II (solid line). The dashed lines stand for the results with the smallest values for the spin-triplet scattering lengths $a_{1/2,1}=1.41 \text{ fm}$ and $a'_{1/2,1}=2.74 + i 1.22 \text{ fm}$. As can be seen when the spin-triplet scattering lengths decrease the description of the experimental scattering cross sections is worsened.

Let us first comment on some relevant details about the two-body interactions already reflected in the scattering lengths of Table IV. The 1S_0 ΛN interaction becomes slightly more attractive than the 3S_1 due to the scalar meson exchanges, because the OGE is more repulsive for the spin-triplet than for the spin-singlet partial wave. This is a desirable effect of the 1S_0 and 3S_1 ΛN interactions, because the phase shifts around $p_\Lambda = 200 \text{ MeV}/c$ for few-body calculations of s -shell Λ -hypernuclei are expected to satisfy $\delta(^1S_0) - \delta(^3S_1) \leq 10^\circ$ [14]. It is also interesting to note the strong repulsion appearing in the ΣN system for $(I, J) = (0, 1/2)$ and $(1, 3/2)$ $L = 0$ partial waves. This is a consequence of the presence of an almost forbidden state due to the same symmetry of the spin and isospin wave functions. This is clearly reflected in Table IV in the small value and negative sign of the $a'_{3/2,1}$ and $a'_{1/2,0}$ ΣN scattering lengths as compared to the positive sign and large value of the attractive $a'_{3/2,0}$ and $a'_{1/2,1}$ ΣN scattering lengths. The importance of the $\Lambda N \leftrightarrow \Sigma N$ potential for the ΛNN and ΣNN systems will be discussed at the end of this section.

A. The ΛNN system

Among the four possible S -wave positive parity states, $J = 1/2$ and $3/2$ with isospin $I = 0$ and $I = 1$, those with isospin zero are the more interesting ones. The $I = 0$, $J^P = 1/2^+$ is the channel where the hypertriton lies, while the $I = 0$, $J^P = 3/2^+$ seems to be also attractive. The possibility whether states of total isospin and total angular momentum other than $(I, J) = (0, 1/2)$ could be also bound [15] will be investigated by studying the most natural candidates $(I, J) = (0, 3/2)$, $(1, 1/2)$, and $(1, 3/2)$.

The very weak binding energy of the hypertriton leads one to expect that the wave function is mostly a deuteron surrounded by a distant Λ particle. As a consequence, since the Λ particle is far apart from the two-nucleon subsystem, the on-shell properties of the ΛN and ΣN interactions are expected to be well reflected. In particular, this system is very well suited to learn about the relative strength of the 1S_0 and 3S_1 attraction of the ΛN interaction. The 1S_0 component plays a more important role than the 3S_1 in the hypertriton, although the available low-energy Λp total cross section data cannot discriminate among the different combinations of the two S -wave interactions.

Let us first present the results for the isospin-0 channels. We show in Table V the results obtained from the various cases of Table IV. For the channel with total spin $3/2$ we give the scattering length, $A_{0,3/2}$, while for the channel with total spin $1/2$ we give the low-energy parameters, $A_{0,1/2}$ and $R_{0,1/2}$, as well as the hypertriton binding energy, $B_{0,1/2}$. Since the binding energy is very small the effective range, $R_{0,1/2}$, has been obtained from the binding energy and the scattering length using the relation,

$$R_{0,1/2} = (\sqrt{2\mu_{\Lambda d}B_{0,1/2}} + 1/A_{0,1/2})/(\mu_{\Lambda d}B_{0,1/2}). \quad (25)$$

We observe how the increase of the three-body system binding energy implies that the effective range of the interaction becomes smaller, the essence of the variational argument made in Ref. [16] to show that the nuclear force must have a finite (nonzero) range or the triton would collapse to a point.

As one can see in Table V the values for the spin- $3/2$ scattering length, $A_{0,3/2}$, are very large, which means that there is a pole very near threshold. Moreover, in some cases it becomes negative. This would imply that the pole is a bound state of which there is no experimental evidence whatsoever. Since in the $(I, J) = (0, 3/2)$ channel the hyperon-nucleon interaction with spin-singlet does not contribute this means those cases producing a $(0, 3/2)$ bound state have too much attraction in the spin-triplet hyperon-nucleon interaction. This can be easily checked in Table IV noting that the bound state appears when increasing the $a_{1/2,1}$ scattering length, the result being independent of the $a_{1/2,0}$ scattering length. We plot in Fig. 2 the inverse of the Λd scattering length, $1/A_{0,3/2}$, as a function of the ΛN spin-triplet scattering length, $a_{1/2,1}$, for all cases in Table IV, which as one sees falls within a smooth curve. From this figure one sees that a bound state will appear if $a_{1/2,1}$ is larger than 1.68 fm. Thus, if we impose the condition that the $(I, J) = (0, 3/2)$ bound state should not appear we find that the scattering length of the ΛN $(i, j) = (1/2, 1)$ channel must be smaller than 1.68 fm. Moreover, we found in Fig. 1 that the fit of the hyperon-nucleon cross sections is worsened for those cases where the spin-triplet ΛN scattering length is smaller than 1.41 fm, so that we conclude that $1.41 \leq a_{1/2,1} \leq 1.68$ fm. From Table IV one can estimate ranges of validity for the other ΛN and ΣN scattering lengths.

The spin $1/2$ scattering length, $A_{0,1/2}$, is negative since there is a bound state in this channel (the hypertriton). The experimental value of the hypertriton binding energy is 0.13 ± 0.05 MeV and, as it can be seen in Table V, the results of all models are consistent with the experimental value. We plot in Fig. 3 the low-energy parameters $R_{0,1/2}$ and $A_{0,1/2}$ as a function of the hypertriton binding energy for the different models of Table IV where as one can see they both fall within smooth curves. Our model gives a hypertriton binding energy of 0.124 MeV, and the low-energy parameters have the values $R_{0,1/2} = 3.82$ fm and $A_{0,1/2} = -17.2$ fm.

Finally, let us consider the isospin-1 channels. We show in Fig. 4 the Fredholm determinant of the $(I, J) = (1, 1/2)$ and $(1, 3/2)$ channels for energies below the ΛNN threshold. The channel $(1, 1/2)$ is attractive but not enough to produce a bound state (i.e., the Fredholm determinant does not cross the negative real axis) while the channel $(1, 3/2)$ is repulsive. The results for the other cases in Table IV are very similar to those of Fig. 4. Let us finally say that the ΛNN channels could be ordered by the strength of their attraction in the following way $(0, 1/2) \geq (0, 3/2) \geq (1, 1/2) \geq (1, 3/2)$. A similar conclusion was obtained in the simultaneous study of the $\Lambda(\Sigma)NN$ systems of Ref. [15] using the Nijmegen hyperon-nucleon and realistic NN interactions.

Considering altogether the $J = 1/2$ and $J = 3/2$ ΛNN channels, information about the relative contribution of the 1S_0 and $^3S_1 - ^3D_1$ hyperon-nucleon forces can be obtained. As explained above the nonexistence of a $J = 3/2$ ΛNN bound state provides with an upper limit to the value of the spin-triplet ΛN scattering length. The remaining contribution to the hypertriton binding energy comes from the spin-singlet partial wave. When the hypertriton is correctly described, the contribution to the Λp scattering cross section of the spin-singlet and spin-triplet partial waves is comparable and they are not in the ratio 3 : 1 as could be expected. This ratio for their relative contribution would either overestimate the Λp scattering cross section or underestimate the hypertriton binding energy.

B. The ΣNN system

While the existence of strangeness -1 Λ -hypernuclei is well established from the observation of many bound states, such has not been the case for Σ -hypernuclei. In the late 80's experiments on the recoilless production of p -shell hypernuclei [17] seemed to indicate the existence of structures that might correspond to unbound states near threshold. Higher statistic experiments were not able to reproduce those earlier peaks, concluding that they were fluctuations in poor statistics [18]. However, there had been a KEK $K^- \rightarrow \pi^-$ at rest experiment on ^4He giving a small ^4_2He peak [19]. In flight $K^- \rightarrow \pi^-$ experiments at 600 MeV/c with high statistics [20] found that this peak was more convincingly prominent, establishing this one ^4_2He Σ -hypernucleus. The possible existence of bound states or resonances of Σ 's in nuclei has become one of the main objectives of the FINUDA Collaboration in DAFNE [21] as well as the KEK laboratory [22], although the interpretation of the results is under discussion [23].

We show in Table VI the Σd scattering lengths $A'_{1,3/2}$ and $A'_{1,1/2}$ for all cases in Table IV. The Σd scattering lengths are complex since the inelastic ΛNN channels are always open. The scattering length $A'_{1,3/2}$ depends only on the spin-triplet hyperon-nucleon channels and both its real and imaginary parts increase when the spin-triplet hyperon-nucleon scattering length increases. Our model, reproducing the experimental hypertriton binding energy, gives $A'_{1,3/2} = 0.36 + i 0.29$ fm. The scattering length $A'_{1,1/2}$ has a negative real part which means that there is a quasibound state very near the Σd threshold in the $(I, J) = (1, 1/2)$ channel. The possible existence of a ΣNN hypertriton bound state or resonance has already being discussed in the literature [24] and the actual possibilities for the experimental study at KEK and FINUDA of this system claims for an experimental effort to look for its possible existence.

We show in Fig. 5 the real part of the Fredholm determinant of the six (I, J) ΣNN channels that are possible for energies below the Σd threshold. The imaginary part of the Fredholm determinant is small and uninteresting. As one can see the channel $(1, 1/2)$ is the most attractive one since the Fredholm determinant is close to zero at the Σd threshold, which as mentioned before, indicates the presence of a quasibound state. The next channel, in what to amount of attraction is concerned, is the $(0, 1/2)$. The states generated by our model have widths of about 0.5 MeV.

Let us make a brief comment on the comparison with our previous results for the ΣNN system published in Ref. [7]. In that work we only worried about the ΣNN system and we adjusted the experimental cross sections using the same scalar exchange for the different spin channels, a naive generalization of the simple $SU(2)$ linear realization of chiral symmetry. The amount of attraction was controlled by means of the harmonic oscillator parameter of the strange quark, $b_s = 0.7$ fm. This procedure does modify all the interactions simultaneously, gluons, pions, etc. increasing the amount of attraction in some cases by reducing the global strength of the repulsive gluon or pion exchanges. The inclusion of the $SU(3)$ scalar mesons gives a different strength for the attraction of the different spin channels and allows to use a more conventional harmonic oscillator parameter for the strange quark, $b_s = 0.55$ fm. Our former calculation had therefore a too attractive spin-singlet hyperon-nucleon interaction and a too repulsive spin-triplet. When studying the ΛNN system it would give a reasonable hypertriton binding energy but a too large Λp elastic cross section. This detailed balance between the spin-singlet and spin-triplet hyperon-nucleon strength, provided naively by the $SU(3)$ scalar quark-meson exchange (see Table II), can only be noticed when the full set of observables of the different $\Lambda(\Sigma)NN$ systems are simultaneously considered. Regarding the energy ordering of the different ΣNN $J = 1/2$ isospin channels, our arguments are fully maintained. The order of the two attractive channels can be easily understood by looking at Table III. All the attractive two-body channels in the NN and ΣN subsystems contribute to the $(I, J) = (1, 1/2)$ ΣNN state (the ΣN channels ${}^3S_1(I = 1/2)$ and ${}^1S_0(I = 3/2)$ and the ${}^3S_1(I = 0)$ NN channel), while the $(I, J) = (0, 1/2)$ state does not present contribution from two of them, the ${}^1S_0(I = 3/2)$ ΣN and specially the ${}^3S_1(I = 0)$ NN deuteron channel. Actually, the NN deuteron-like contribution plays an essential role in the binding of the triton [5] and hypertriton [15]. In this last case the presence of the Λ has the effect of reducing the NN attraction with respect to the deuteron case but the $\Lambda \leftrightarrow \Sigma$ conversion compensates this reduction and binds the system as we will see later on.

C. $\Lambda \leftrightarrow \Sigma$ conversion

It has been pointed out the relevance of small admixture of ΣNN components to bind the hypertriton [15] and also for other observables in hypernuclear physics [2]. The contribution of the $\Lambda \leftrightarrow \Sigma$ conversion should be even stronger than $\Delta \leftrightarrow N$ conversion in ordinary nuclei, because it is not suppressed in S -waves and the $\Lambda - \Sigma$ mass difference is much smaller. We have investigated the effect of the $\Lambda \leftrightarrow \Sigma$ conversion both in the ΛNN and in the ΣNN systems. For this purpose we have solved the most interesting ΛNN channels, $(I, J) = (0, 1/2)$ and $(0, 3/2)$, switching off the transition between the ΛN and ΣN subsystems. This excludes ΣNN states between consecutive t operations and one stays therefore always in

the space of ΛNN states. This intermediate transitions from Σ to Λ induce a three-body force together with a dispersive effect. We plot in Fig. 6(a) the Fredholm determinant for both cases. The solid line indicates the result of the full calculation while the dashed one represents the results without $\Lambda \leftrightarrow \Sigma$ conversion. As can be seen the effect of the ΣNN channel for ΛNN is very important. In fact the hypertriton bound state disappears and the ordering between the $J = 1/2$ and $J = 3/2$ channels is reversed.

We have used the same strategy to evaluate the effect of ΛNN channels for the ΣNN system. We have redone the calculation for the most interesting ΣNN channels, $(I, J) = (0, 1/2)$ and $(1, 1/2)$, disconnecting the $\Sigma \leftrightarrow \Lambda$ conversion. The results are shown in Fig. 6(b). Once again the solid lines represent the full calculation and the dashed ones those without $\Sigma \leftrightarrow \Lambda$ conversion. Once the transition between the ΣN and ΛN channels is disconnected neither the character nor the order of these channels is modified. This is in agreement with our former conclusion that the inclusion of ΛNN channels in the calculation of the ΣNN system did not modify the general trend of the results [7].

To firmly establish the relative importance of the conversion we compare in Fig. 6(c) the role of the $\Sigma \leftrightarrow \Lambda$ coupling in the same (I, J) channel, in particular in the channel of the hypertriton $(I, J) = (0, 1/2)$. Some precaution is needed with respect to the x -axis. The results are drawn as a function of the energy below threshold, those of the ΛNN system being referred to the ΛNN threshold and those of the ΣNN system to the ΣNN threshold. As can be seen the effect of the lower ΛNN channel is less important for the heavier one, ΣNN .

IV. SUMMARY

We have solved the Faddeev equations for the ΛNN and ΣNN systems using the hyperon-nucleon and nucleon-nucleon interactions derived from a chiral constituent quark model with full inclusion of the $\Lambda \leftrightarrow \Sigma$ conversion. We present results for the hypertriton binding energy and the Λd and Σd scattering lengths. We also have calculated the elastic and inelastic ΣN and ΛN cross sections. We study consistently the ΣNN system at threshold.

The set of observables studied gives rise to well-defined intervals for the possible values of the two-body ΛN and ΣN scattering lengths. The presence of almost forbidden states in the ΣN system produces observable effects for the sign and magnitude of the ΣN scattering lengths.

The hypertriton turns out to be bound at the experimental binding energy. We have found that the $\Lambda \leftrightarrow \Sigma$ conversion is crucial for the binding of the hypertriton. It is also of interest to note that the contribution of the 1S_0 and $^3S_1 - ^3D_1$ hyperon-nucleon forces to the binding are not in the ratio 3 : 1 as could be expected, but they are comparable. We also found that the flavor dependence of the scalar meson-exchange between quarks, giving rise to different strengths for the 1S_0 and $^3S_1 - ^3D_1$ attraction, becomes crucial for the understanding of the full set of observables studied. From the nonexistence of a ΛNN $(I, J) = (0, 3/2)$ bound state, we derive an upper limit for the spin-triplet ΛN scattering length, and a lower limit can be derived from the correct description of two-body scattering cross sections.

The ΣNN system does not present any bound state. The $(I, J) = (1, 1/2)$ and $(I, J) = (0, 1/2)$ states are the only attractive S -wave channels, the $(I, J) = (1, 1/2)$ with a quasibound state or resonance close above the three-body threshold. The channel with $I = 1$ is always more attractive than the one with $I = 0$. We have also studied the effect of the $\Lambda \leftrightarrow \Sigma$ conversion for the ΣNN system, its effect being much smaller than in the ΛNN channel.

ACKNOWLEDGMENTS

It is a great pleasure to thank Pedro González for a careful reading of the manuscript and challenging and fruitful discussions as well as many suggestions about this work. This work has been partially funded by Ministerio de Educación y Ciencia under Contract No. FPA2004-05616, by Junta de Castilla y León under Contract No. SA-104/04, by Generalitat Valenciana under Contract No. GV05/276, and by COFAA-IPN (México).

REFERENCES

- [1] K. Miyagawa and W. Glöckle, Phys. Rev. C **48**, 2576 (1993).
- [2] A. Nogga, H. Kamada, and W. Glöckle, Phys. Rev. Lett. **88**, 172501 (2002).
- [3] Th.A. Rijken, V.G.J. Stoks, and Y. Yamamoto, Phys. Rev. C **59**, 21 (1999).
- [4] Y. Fujiwara, Y. Suzuki, and C. Nakamoto, Prog. Part. Nucl. Phys. in press (nucl-th/0607013); Y. Fujiwara, K. Miyagawa, M. Kohno, and Y. Suzuki, Phys. Rev. C **70**, 024001 (2004).
- [5] A. Valcarce, H. Garcilazo, F. Fernández, and P. González, Rep. Prog. Phys. **68**, 965 (2005).
- [6] A. Valcarce, H. Garcilazo, and J. Vijande, Phys. Rev. C **72**, 025206 (2005). J. Vijande, F. Fernández, and A. Valcarce, J. Phys. G **31**, 481 (2005).
- [7] T. Fernández-Caramés, A. Valcarce, H. Garcilazo, and P. González, Phys. Rev. C **73**, 034004 (2006).
- [8] W.-M. Yao *et al.*, J. Phys. G **33**, 1 (2006).
- [9] H. Garcilazo, T. Fernández-Caramés, A. Valcarce, and P. González, in preparation.
- [10] G.H. Berthold, H. Zankel, L. Mathelitsch, and H. Garcilazo, Il Nuovo Cimento **93 A**, 89 (1986).
- [11] G. Alexander *et al.*, Phys. Rev. **173**, 1452 (1968).
- [12] F. Eisele, H. Filthuth, W. Fölisch, V. Hepp, E. Leitner, and G. Zetch, Phys. Lett. **37**, 204 (1971).
- [13] R. Engelmann, H. Filthuth, V. Hepp, and E. Kluge, Phys. Lett. B **21**, 587 (1966).
- [14] K. Miyagawa and H. Yamamura, Phys. Rev. C **60**, 024003 (1999).
- [15] K. Miyagawa, H. Kamada, W. Glöckle, and V. Stoks, Phys. Rev. C **51**, 2905 (1995).
- [16] L.H. Thomas, Phys. Rev. **47**, 903 (1935). H.A. Bethe and R.F. Bacher, Rev. Mod. Phys. **8**, 82 (1936).
- [17] T. Yamazaki *et al.*, Phys. Rev. Lett. **54**, 102 (1985).
- [18] S. Bart *et al.*, Phys. Rev. Lett. **83**, 5238 (1999).
- [19] R.S. Hayano *et al.*, Phys. Lett. B **231**, 355 (1989).
- [20] T. Nagae *et al.*, Phys. Rev. Lett. **80**, 1605 (1998).
- [21] FINUDA Collaboration, S. Piano, Czechoslovak J. Phys. **52**, B193 (2002).
- [22] T. Suzuki *et al.*, Phys. Lett. B **597**, 263 (2004). T. Suzuki *et al.*, Nucl. Phys. A **754**, 375 (2005). M. Iwasaki *et al.*, nucl-ex/0310018.
- [23] E. Oset and H. Toki, Phys. Rev. C **74**, 015207 (2006).
- [24] I.R. Afnan and B.F. Gibson, Phys. Rev. C **47**, 1000 (1993).

TABLES

TABLE I. Expectation value of the different scalar meson-exchange flavor operators.

O_{ij}	$\langle N\Lambda O_{ij} N\Lambda \rangle$		$\langle N\Sigma O_{ij} N\Sigma \rangle$				$\langle N\Lambda O_{ij} N\Sigma \rangle$	
	$I = 1/2$		$I = 1/2$		$I = 3/2$		$I = 1/2$	
	$S = 0$	$S = 1$	$S = 0$	$S = 1$	$S = 0$	$S = 1$	$S = 0$	$S = 1$
$\sum_{F=1}^3 \lambda_3^F \cdot \lambda_6^F$	0	0	-4/9	-4/9	2/9	2/9	0	0
$\sum_{F=4}^7 \lambda_3^F \cdot \lambda_6^F$	1/3	-1/3	-1/9	1/9	2/9	-2/9	1/3	-1/3
$\lambda_3^8 \cdot \lambda_6^8$	0	0	0	0	0	0	0	0
$\lambda_3^0 \cdot \lambda_6^0$	2/3	2/3	2/3	2/3	2/3	2/3	2/3	2/3

TABLE II. Parameters, in fm^{-1} , of the scalar meson-exchange potential in Eq. (3).

Spin	m_s	Λ_s
0	3.73	4.2
1	4.12	5.2

TABLE III. Two-body ΣN channels (i_Σ, s_Σ), ΛN channels (i_Λ, s_Λ), NN channels with Σ spectator ($i_{N(\Sigma)}, s_{N(\Sigma)}$), and NN channels with Λ spectator ($i_{N(\Lambda)}, s_{N(\Lambda)}$) that contribute to a given $\Sigma NN - \Lambda NN$ state with total isospin I and spin J .

I	J	(i_Σ, s_Σ)	(i_Λ, s_Λ)	$(i_{N(\Sigma)}, s_{N(\Sigma)})$	$(i_{N(\Lambda)}, s_{N(\Lambda)})$
0	1/2	(1/2,0),(1/2,1)	(1/2,0),(1/2,1)	(1,0)	(0,1)
1	1/2	(1/2,0),(3/2,0),(1/2,1),(3/2,1)	(1/2,0),(1/2,1)	(0,1),(1,0)	(1,0)
2	1/2	(3/2,0),(3/2,1)		(1,0)	
0	3/2	(1/2,1)	(1/2,1)		(0,1)
1	3/2	(1/2,1),(3/2,1)	(1/2,1)	(0,1)	
2	3/2	(3/2,1)			

TABLE IV. ΛN scattering lengths, $a_{1/2,0}$ and $a_{1/2,1}$, and ΣN scattering lengths, $a'_{1/2,0}$, $a'_{1/2,1}$, $a'_{3/2,0}$, and $a'_{3/2,1}$ (in fm), dependence on the strength of the spin-singlet and spin-triplet scalar interaction. Masses are in fm^{-1} . The values in parenthesis under the first row correspond to the scattering lengths obtained using the expansion (7) with $0 \leq n \leq 11$.

$m_s(S=0)$	$m_s(S=1)$	$a_{1/2,0}$	$a_{1/2,1}$	$a'_{1/2,0}$	$a'_{1/2,1}$	$a'_{3/2,0}$	$a'_{3/2,1}$
3.73	4.12	2.48	1.65	$-0.66+i0.12$	$3.20+i1.52$	3.90	-0.42
		(2.50)	(1.67)	($-0.64+i0.12$)	($3.24+i1.52$)	(3.96)	(-0.40)
3.76	4.12	2.31	1.65	$-0.66+i0.12$	$3.20+i1.52$	3.64	-0.42
3.71	4.12	2.55	1.65	$-0.65+i0.12$	$3.20+i1.52$	4.20	-0.42
3.68	4.12	2.74	1.65	$-0.65+i0.12$	$3.20+i1.52$	4.72	-0.42
3.73	4.20	2.48	1.41	$-0.66+i0.12$	$2.74+i1.22$	3.90	-0.44
3.73	4.10	2.48	1.72	$-0.66+i0.12$	$3.34+i1.62$	3.90	-0.42
3.73	4.08	2.48	1.79	$-0.66+i0.12$	$3.48+i1.72$	3.90	-0.41
3.73	4.06	2.48	1.87	$-0.66+i0.12$	$3.64+i1.85$	3.90	-0.41
3.73	4.04	2.48	1.95	$-0.66+i0.12$	$3.81+i1.98$	3.90	-0.40

TABLE V. Ad scattering lengths, $A_{0,3/2}$ and $A_{0,1/2}$, effective range, $R_{0,1/2}$ (in fm), and hypertriton binding energy $B_{0,1/2}$ (in MeV) for all cases of Table IV

$m_s(S=0)$	$m_s(S=1)$	$A_{0,3/2}$	$A_{0,1/2}$	$R_{0,1/2}$	$B_{0,1/2}$
3.73	4.12	198.2	-17.2	3.82	0.124
3.76	4.12	198.2	-22.4	4.47	0.070
3.71	4.12	198.2	-16.8	3.80	0.130
3.68	4.12	198.2	-14.4	3.51	0.182
3.73	4.20	66.3	-20.0	4.17	0.089
3.73	4.10	-179.8	-16.6	3.75	0.134
3.73	4.08	-62.7	-16.0	3.68	0.145
3.73	4.06	-38.2	-15.4	3.61	0.156
3.73	4.04	-27.6	-14.9	3.55	0.168

TABLE VI. Σd scattering lengths, $A'_{1,3/2}$ and $A'_{1,1/2}$ (in fm), for all cases in Table IV.

$m_s(S=0)$	$m_s(S=1)$	$A'_{1,3/2}$	$A'_{1,1/2}$
3.73	4.12	$0.36+i 0.29$	$-1.55+i 42.31$
3.76	4.12	$0.36+i 0.29$	$14.95+i 31.61$
3.71	4.12	$0.36+i 0.29$	$-21.04+i 33.19$
3.68	4.12	$0.36+i 0.29$	$-23.29+i 13.32$
3.73	4.20	$0.20+i 0.26$	$19.28+i 25.37$
3.73	4.10	$0.40+i 0.30$	$-10.47+i 40.25$
3.73	4.08	$0.44+i 0.31$	$-17.33+i 35.01$
3.73	4.06	$0.49+i 0.33$	$-21.16+i 28.54$
3.73	4.04	$0.54+i 0.34$	$-22.44+i 22.44$

FIGURES

FIG. 1. Calculated ΛN , ΣN and $\Sigma N \rightarrow \Lambda N$ total cross sections compared with experimental data. Experimental data in (a) are from Ref. [11], in (b) and (c) are from Ref. [12], and in (d) and (e) from Ref. [13].

FIG. 2. The inverse of the $(I, J) = (0, 3/2)$ Λd scattering length as a function of the ΛN $a_{1/2,1}$ scattering length for all models of Table IV. The solid line is to guide the eye.

FIG. 3. The $(I, J) = (0, 1/2)$ Λd scattering length and effective range parameters as a function of the hypertriton binding energy for all models of Table IV. The solid line is to guide the eye.

FIG. 4. Fredholm determinant for the ΛNN channels $(I, J) = (1, 1/2)$ and $(1, 3/2)$ for the model giving the solid line ΣN total cross sections of Fig. 1 and for energies below the ΛNN threshold.

FIG. 5. Fredholm determinant for (a) $J = 1/2$ and (b) $J = 3/2$ ΣNN channels for the model giving the solid line ΣN total cross sections of Fig. 1. The Σd continuum starts at $E = -2.225$ MeV, the deuteron binding energy obtained within our model.

FIG. 6. (a) Fredholm determinant for $J = 1/2$ and $J = 3/2$ $I = 0$ ΛNN channels. The solid line stands for the full calculation and the dashed line when the $\Lambda \leftrightarrow \Sigma$ transition is taken to be zero. (b) Same as (a) for the $I = 0$ and $I = 1$ $J = 1/2$ ΣNN channels. (c) Same as (a) for $(I, J) = (0, 1/2)$ ΛNN and ΣNN channels.

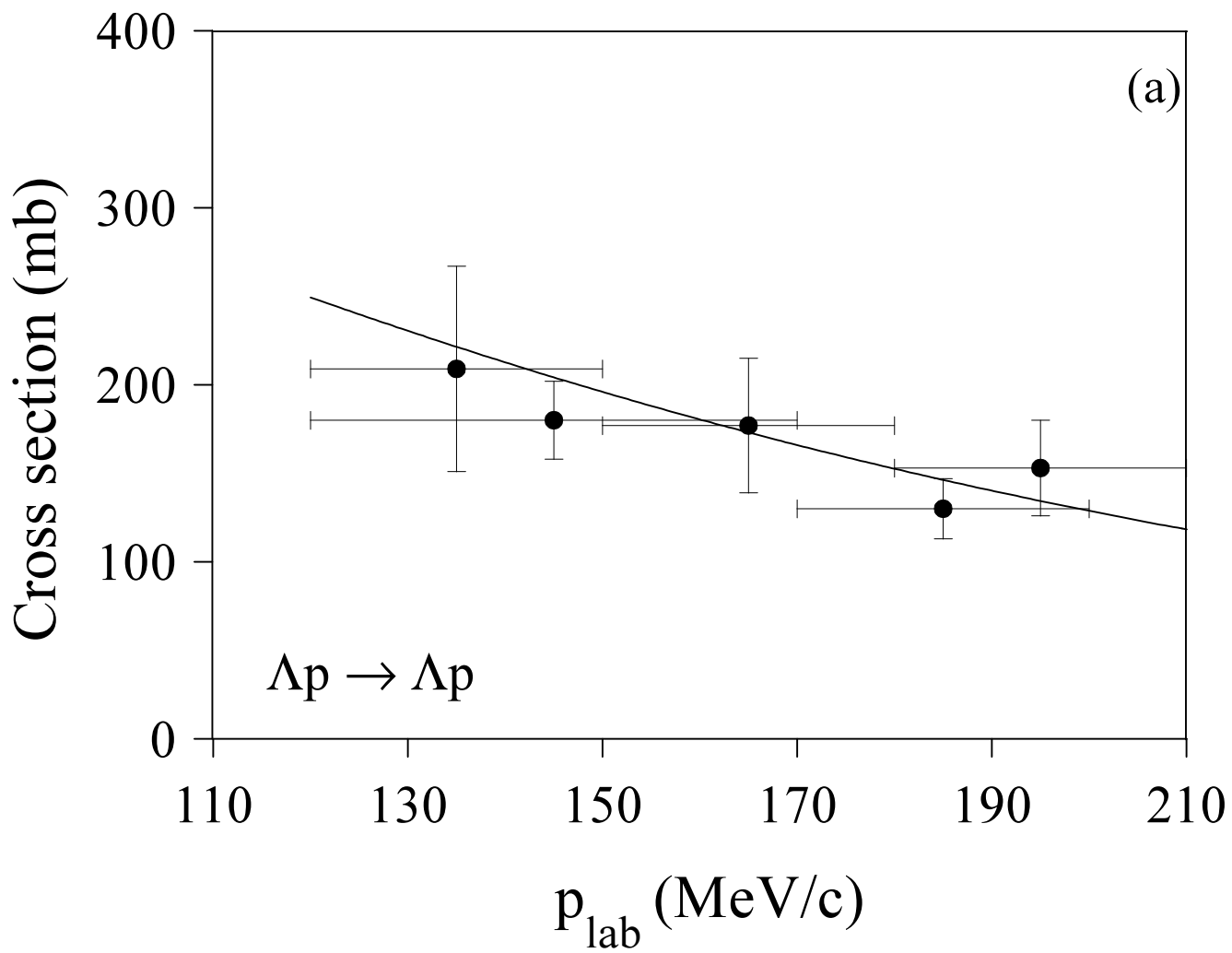


Figure 1

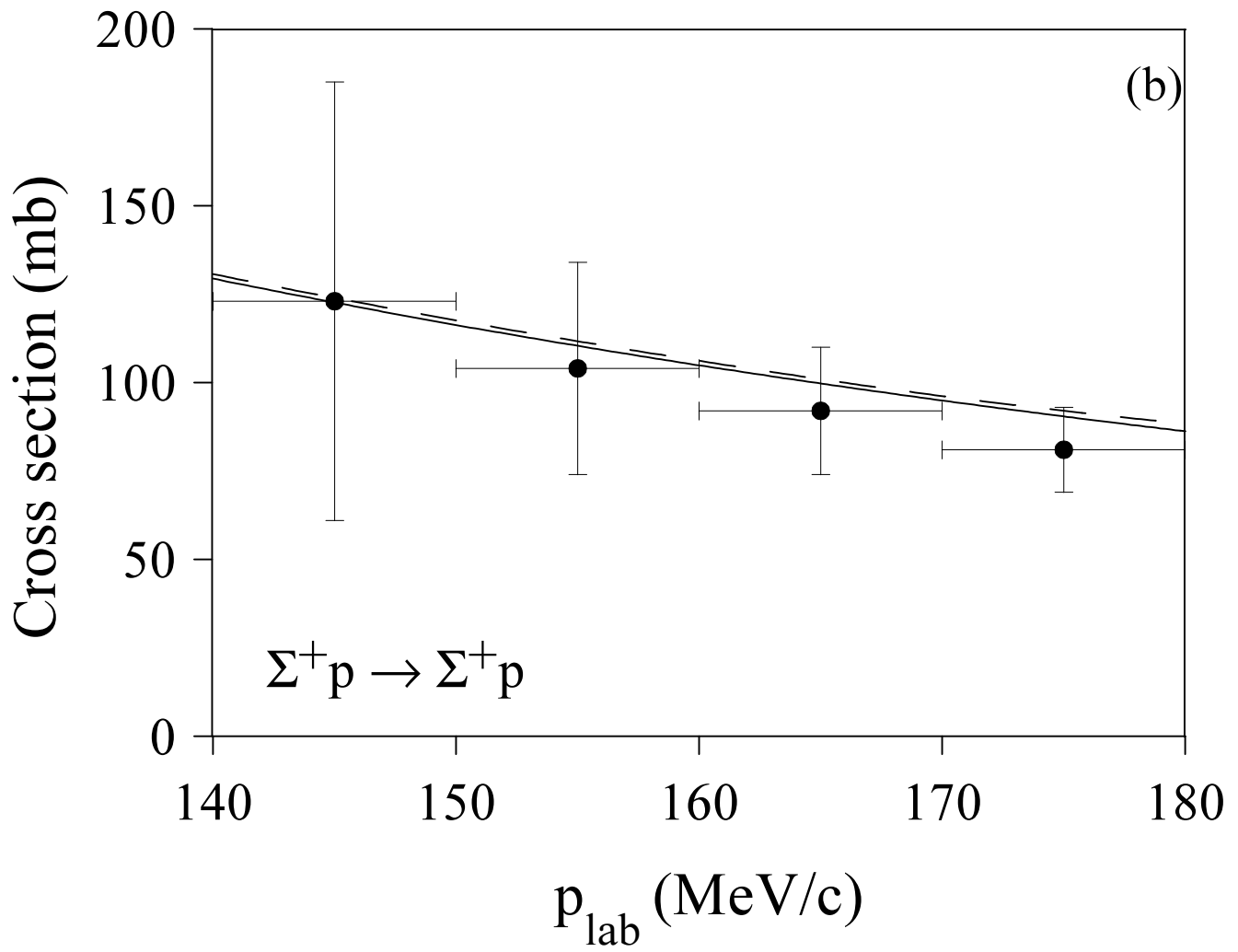


Figure 1

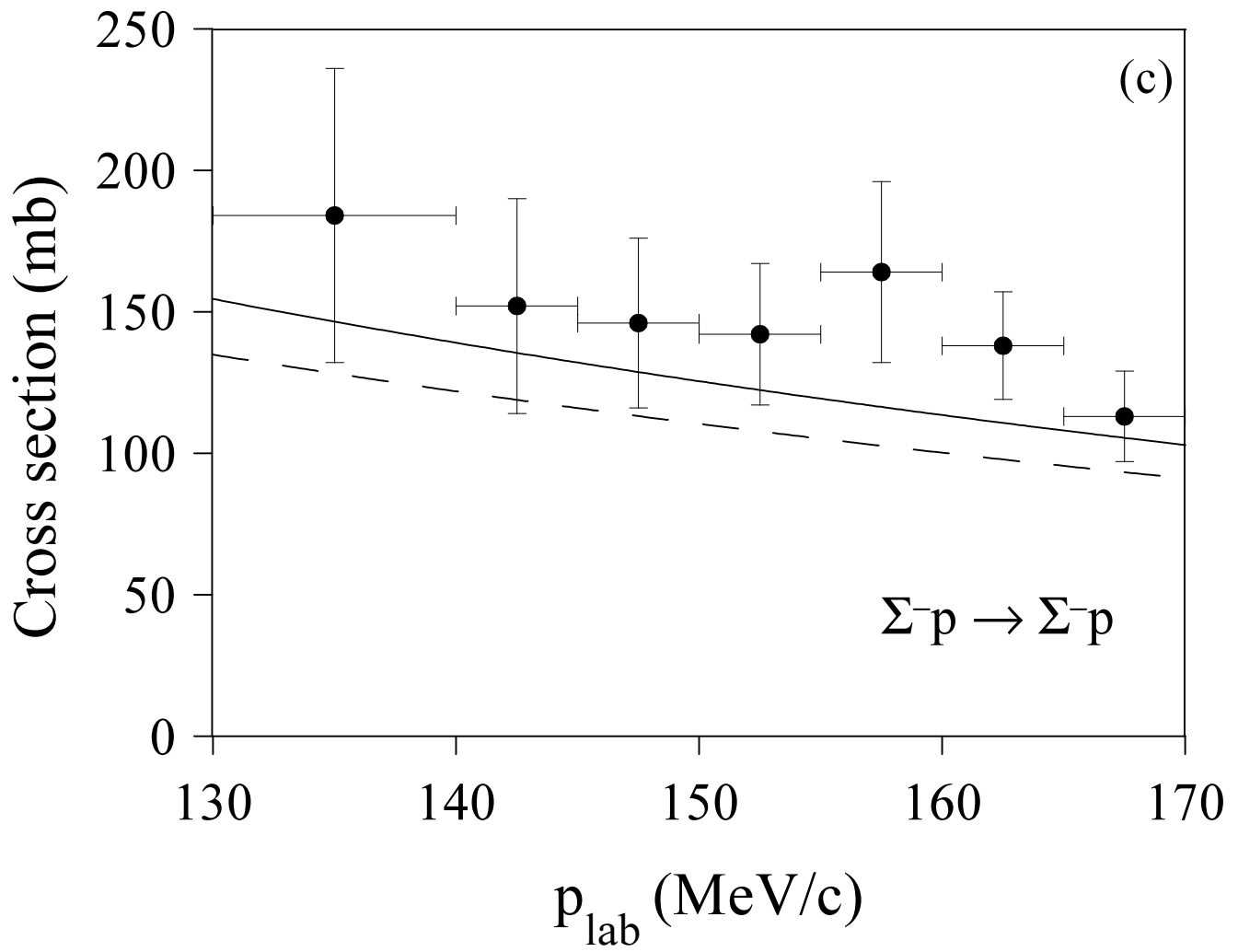


Figure 1

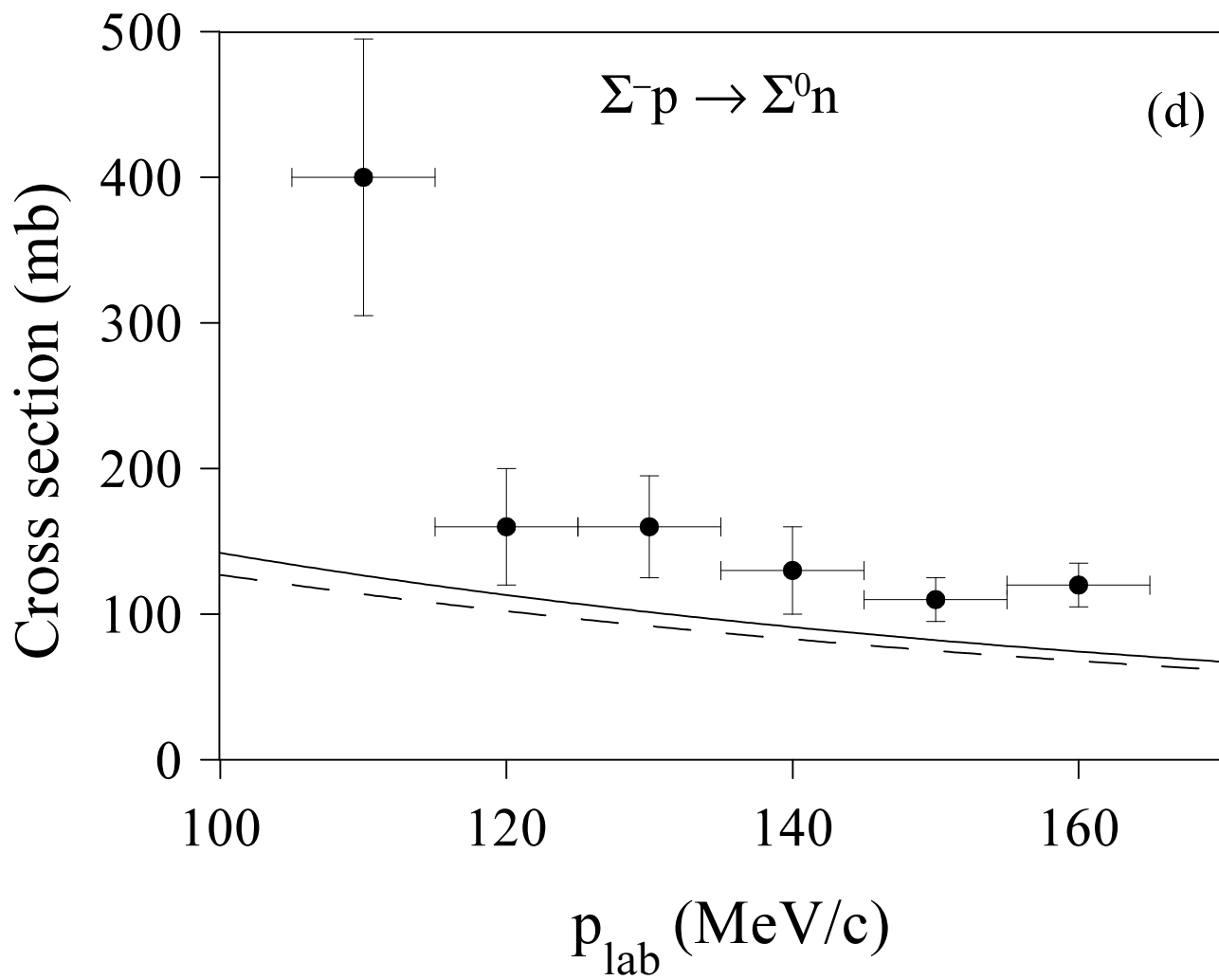


Figure 1

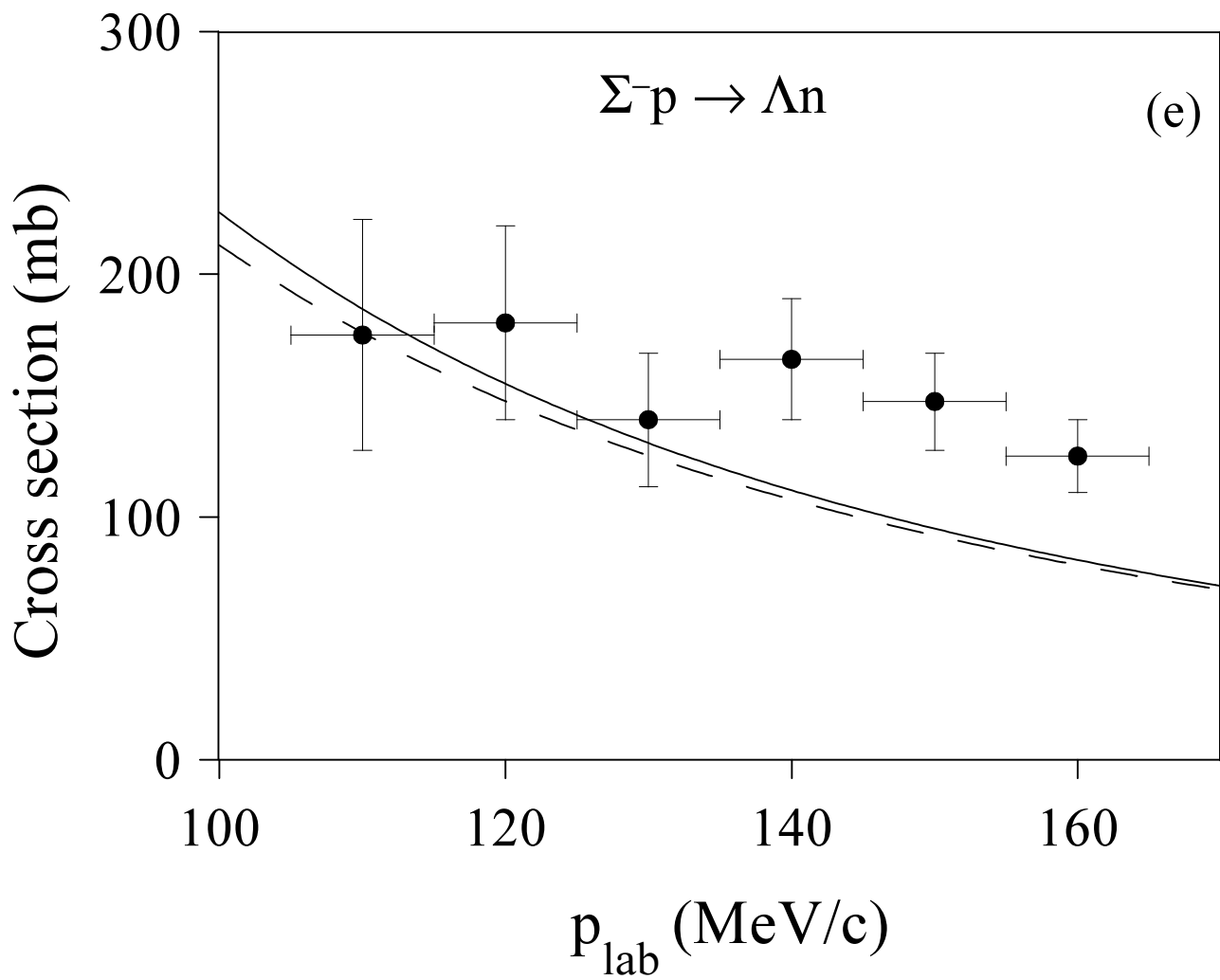


Figure 1

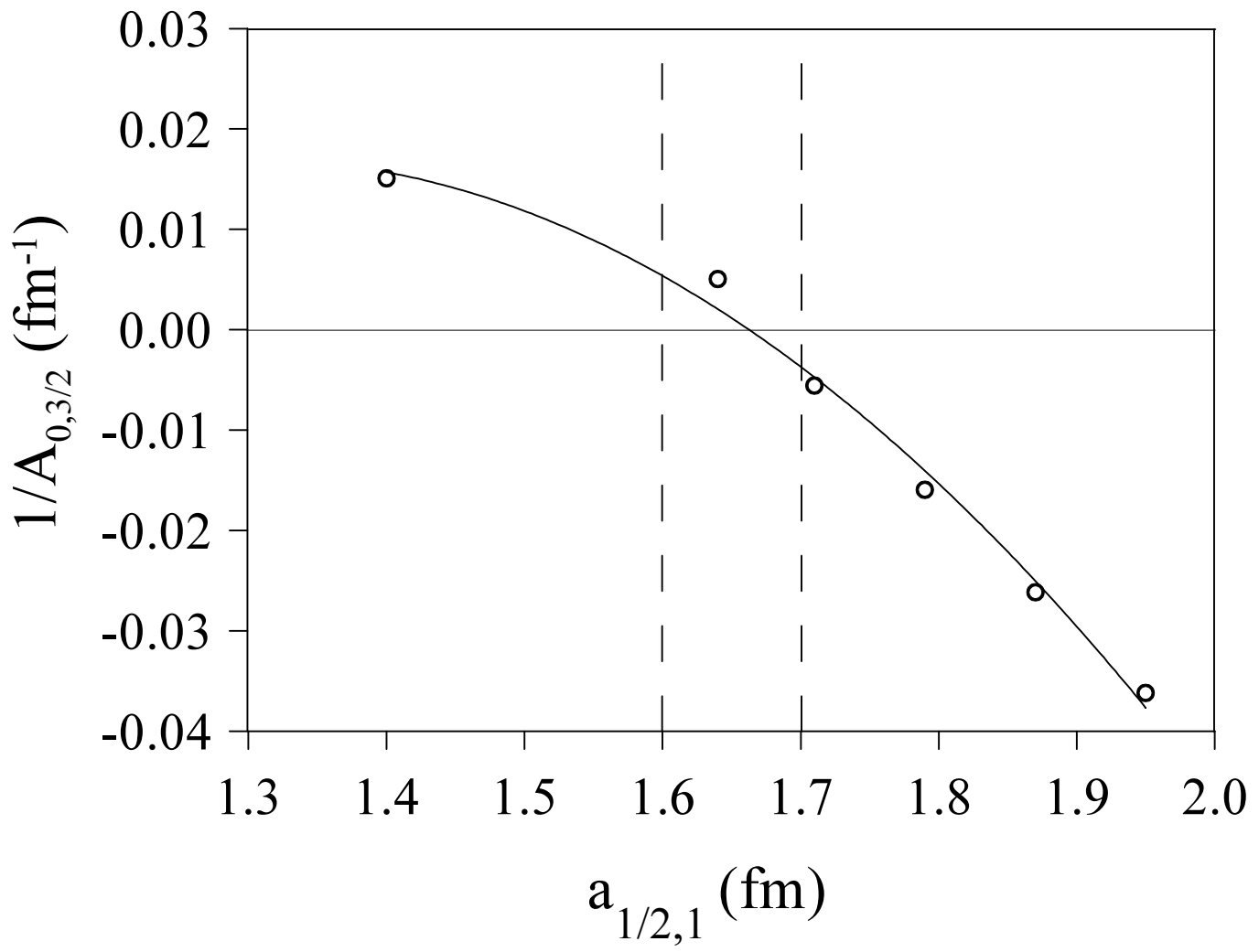


Figure 2

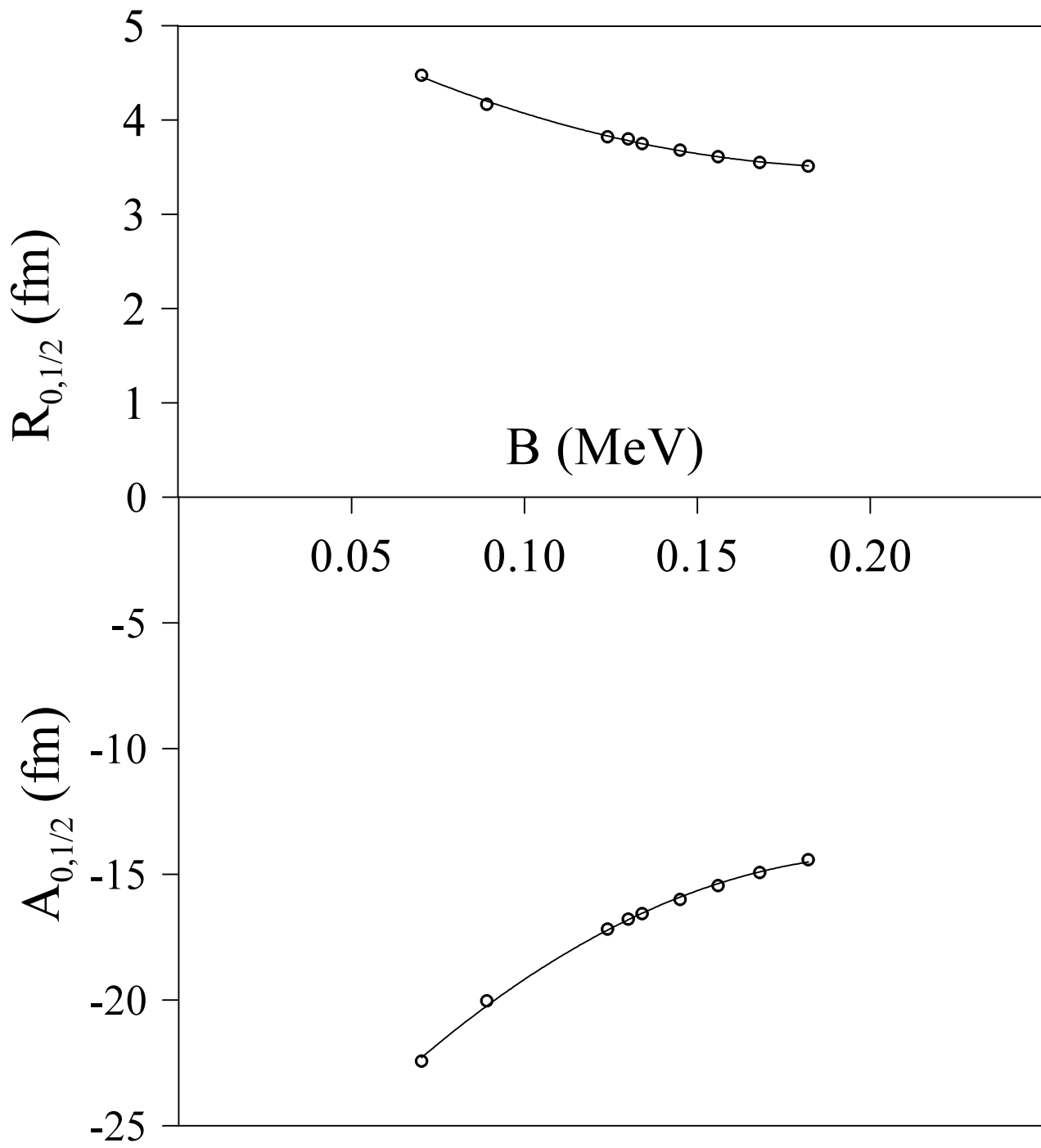


Figure 3

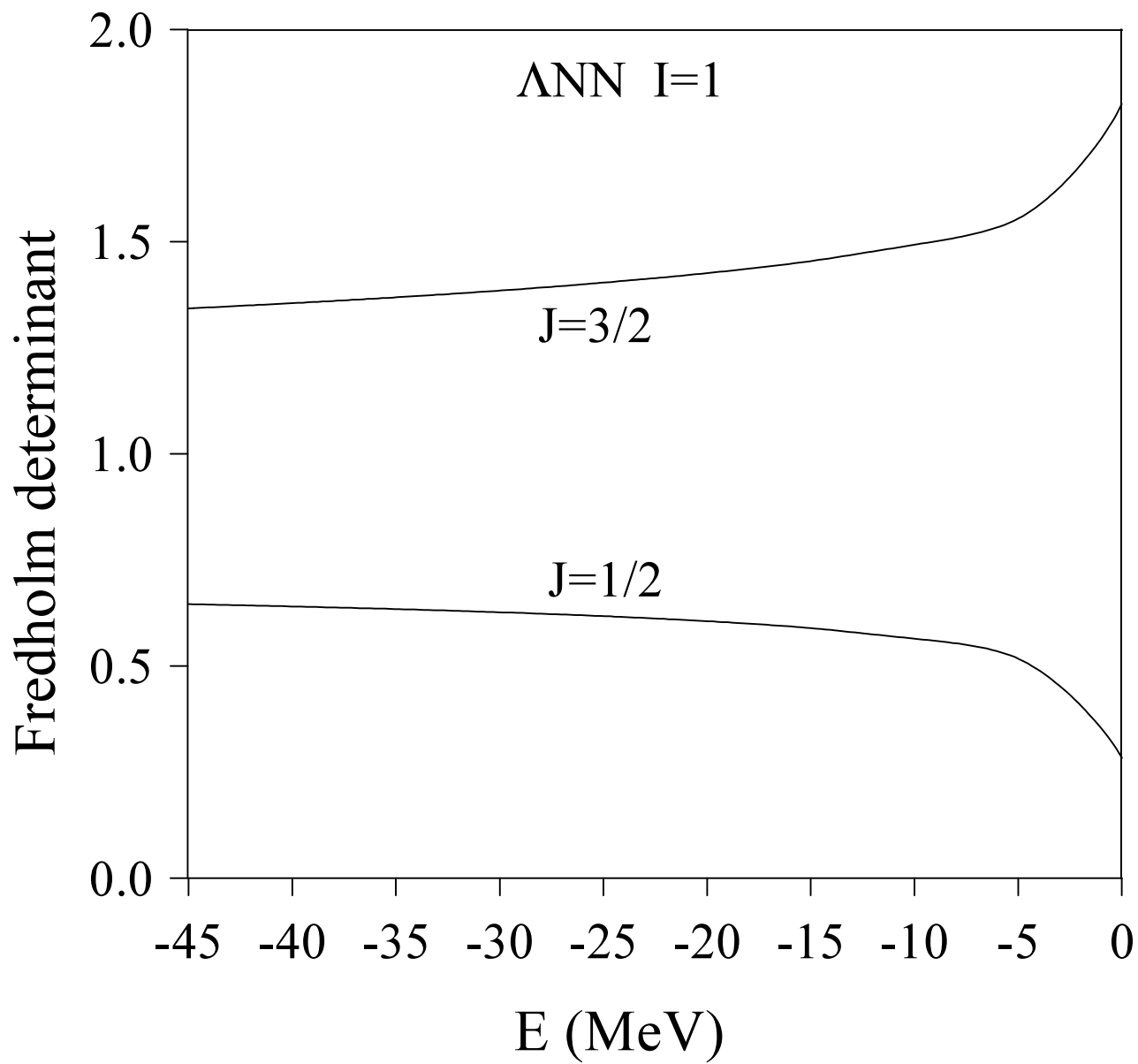


Figure 4

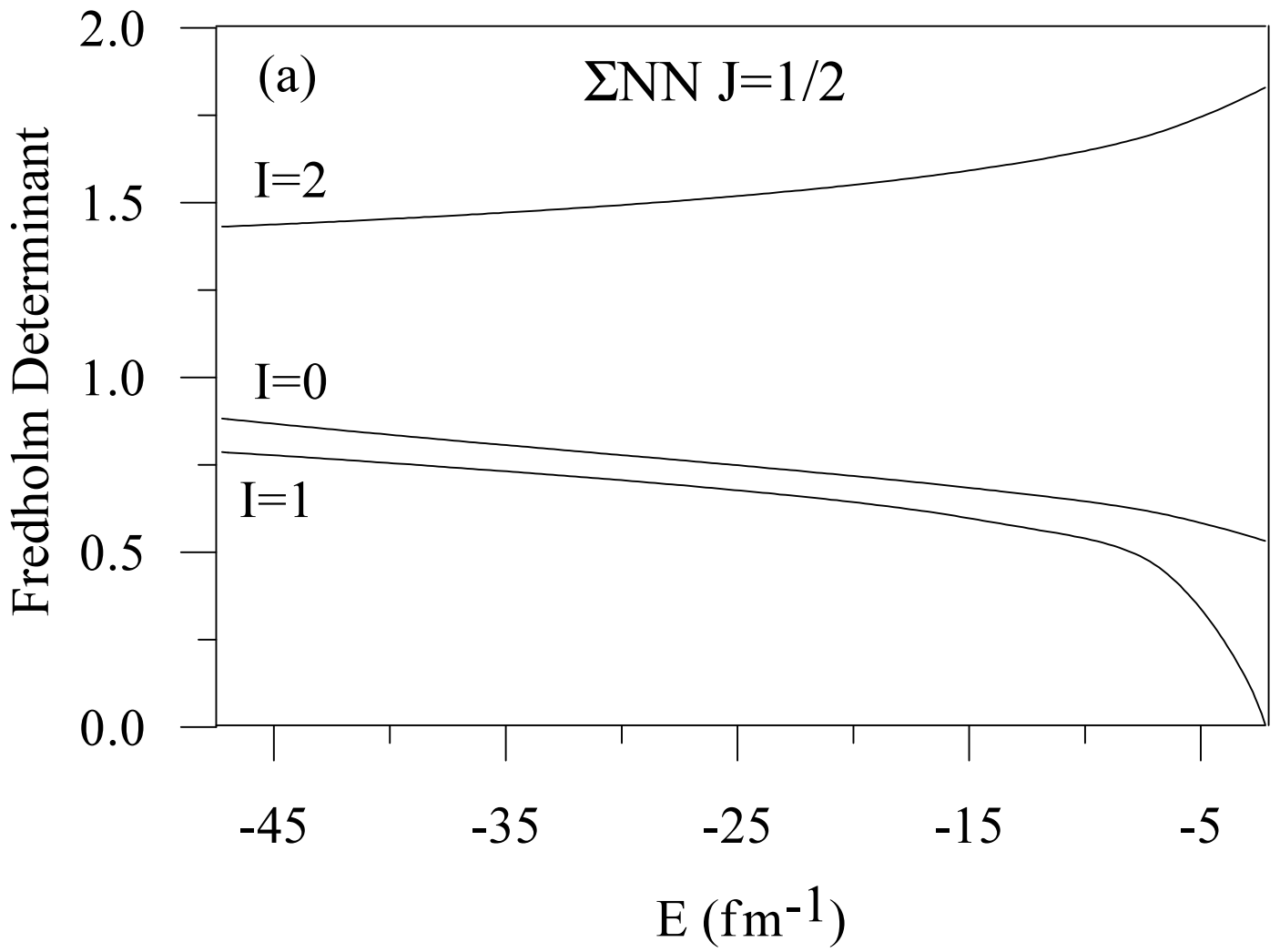


Figure 5

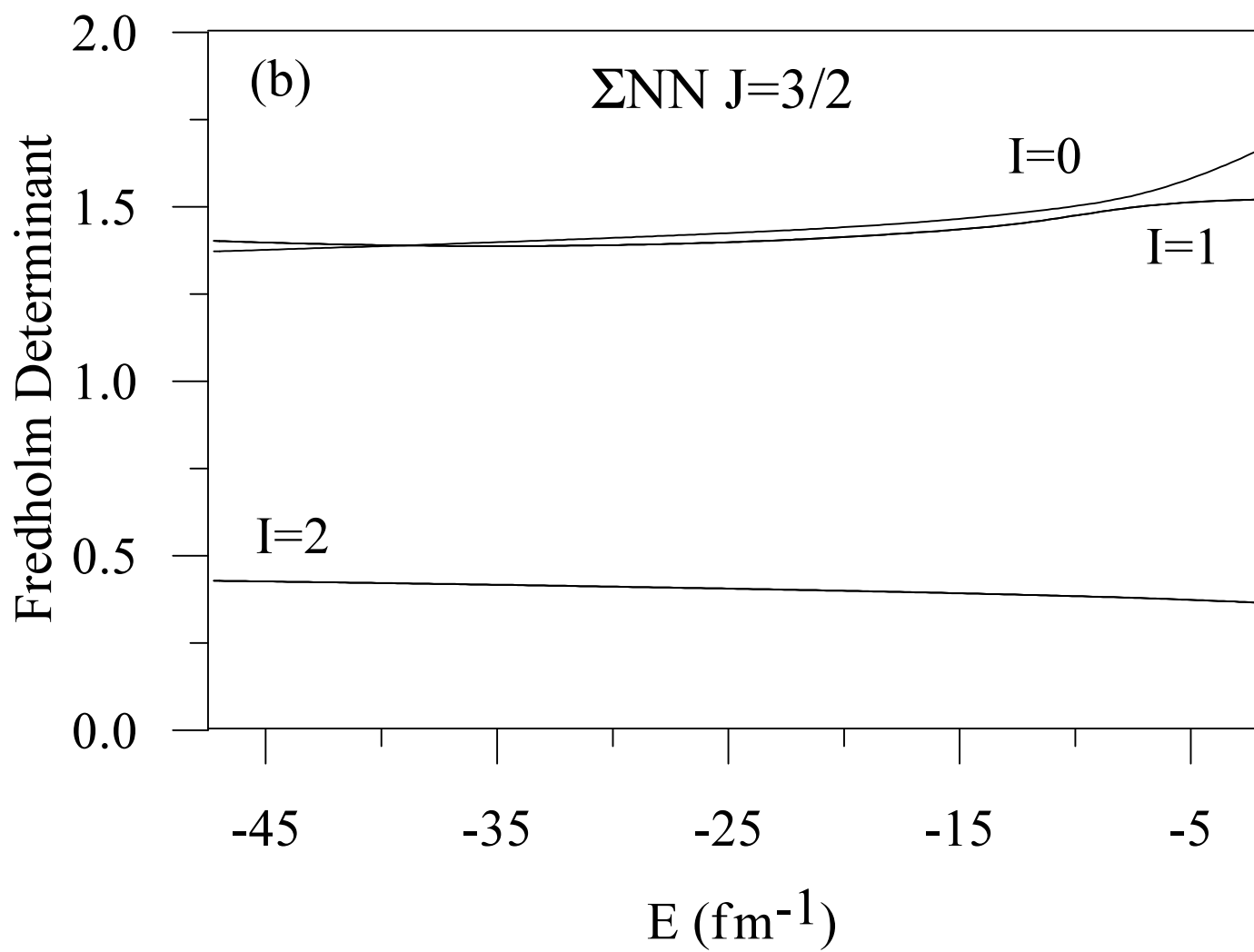


Figure 5

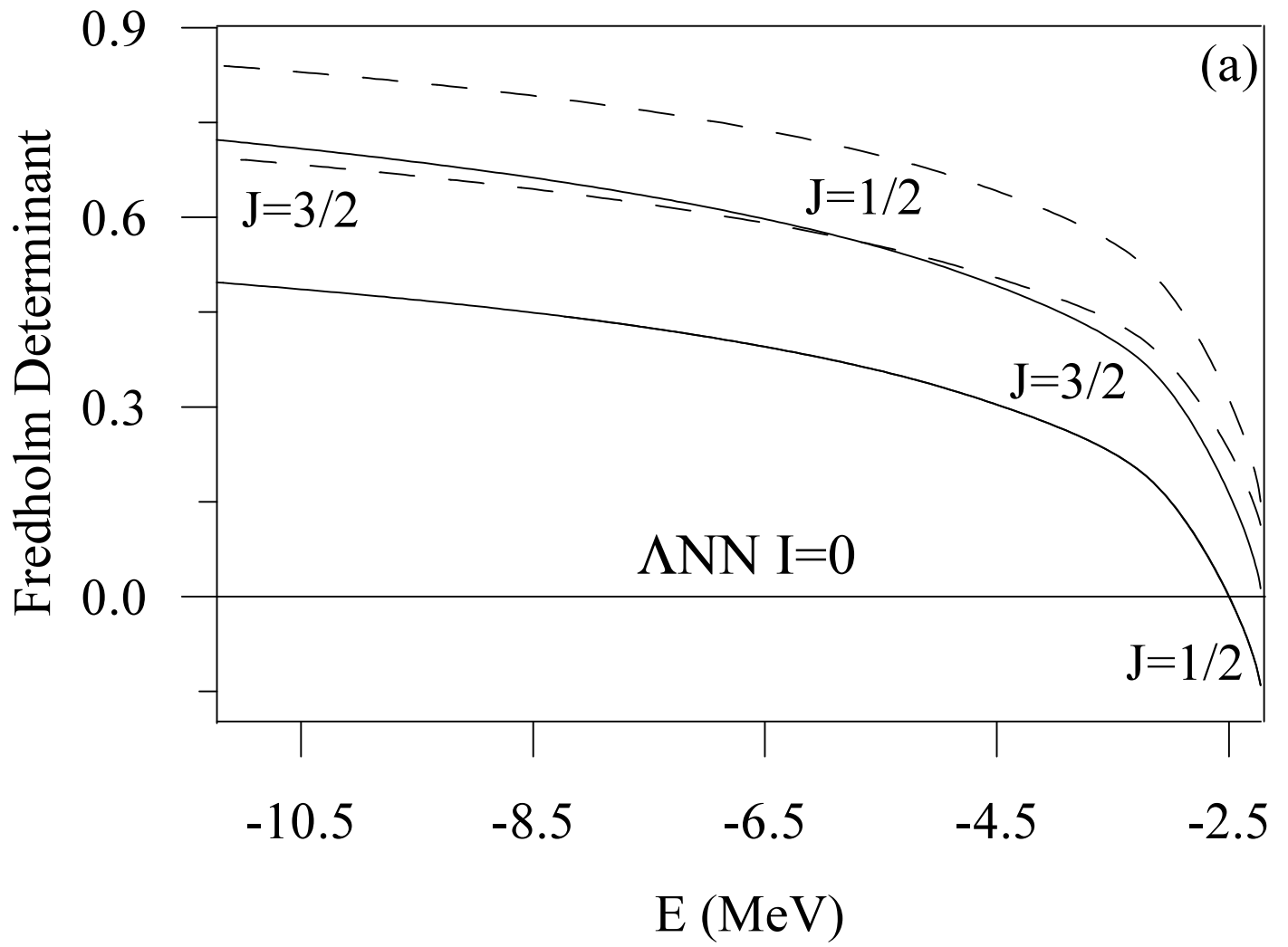


Figure 6

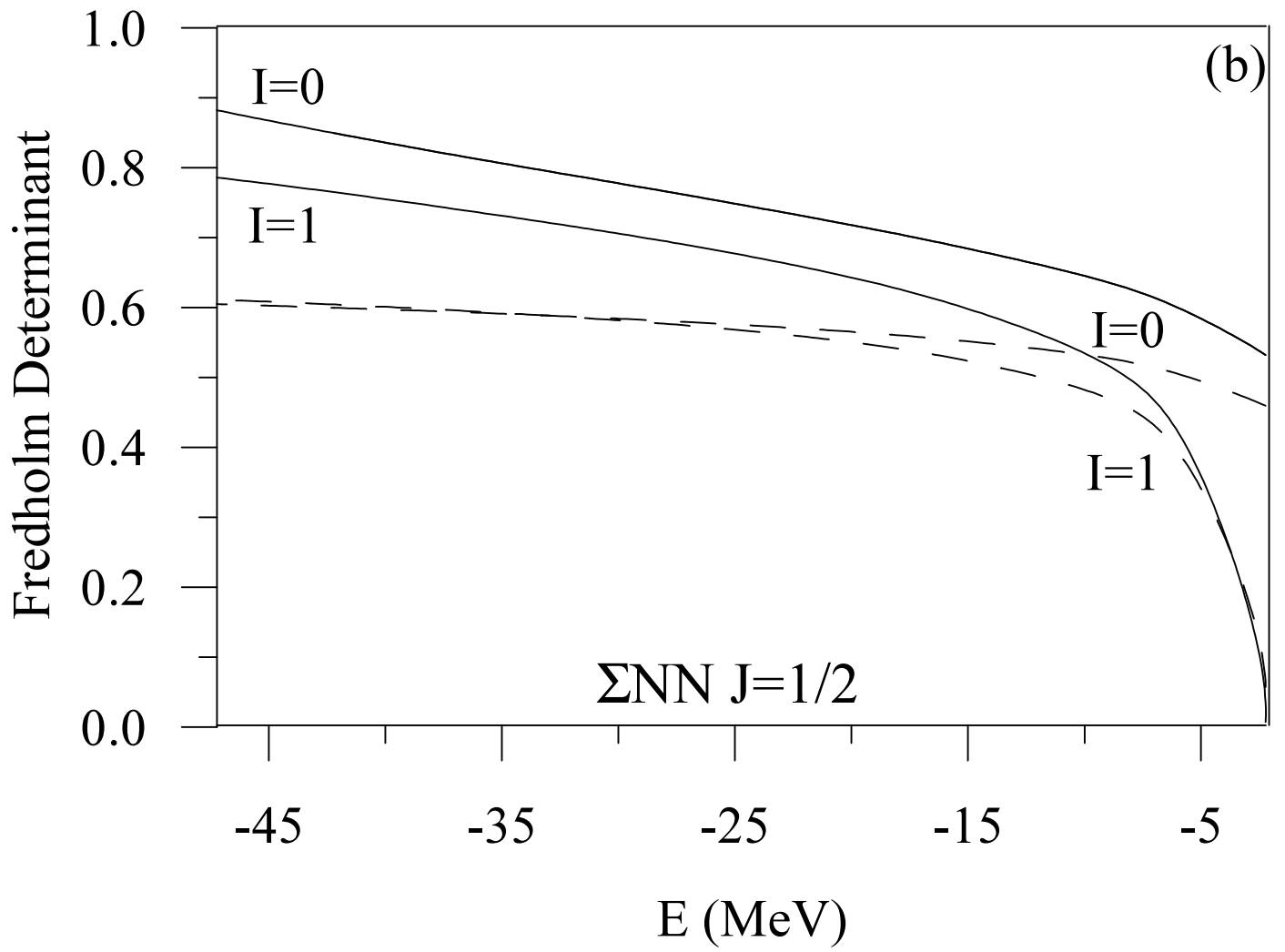


Figure 6

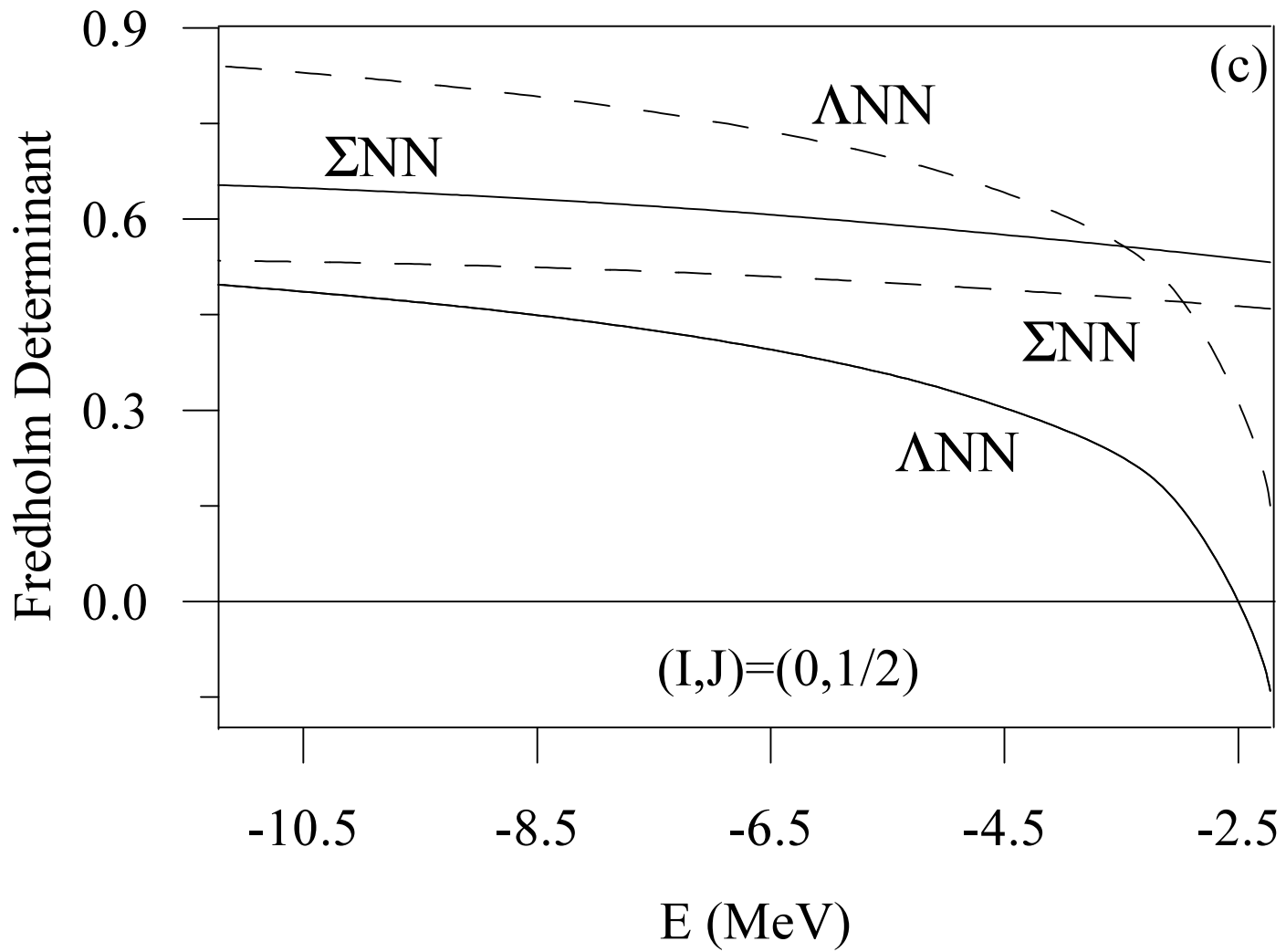


Figure 6